Electronic Supplementary Information

Ultrathin Al_2O_3 bridging layer between CdS and ZnO boosting photocatalytic hydrogen production

Dandan Ma,[a] Zhenyu Wang,[a] Jian-Wen Shi,*,[a] Yajun Zou,[a] Yixuan Lv,[a] Xin Ji,[a] Zhihui Li,[a] Yonghong Cheng,[a] Lianzhou Wang*,[b]

[a] *State Key Laboratory of Electrical Insulation and Power Equipment, Center of Nanomaterials for Renewable Energy, School of Electrical Engineering, Xi'an Jiaotong University, Xi'an 710049, China*

[b] *Nanomaterials Centre, School of Chemical Engineering and AIBN, The University of Queensland, St. Lucia, Brisbane, QLD 4072, Australia*

Corresponding author:

Jian-Wen Shi, E-mail: jianwen.shi@mail.xjtu.edu.cn

Lianzhou Wang, E-mail: l.wang@uq.edu.au

1. Materials

Sodium sulfide ($Na_2S{\cdot}9H_2O$) and cadmium acetate dihydrate ($Cd(CH_3COO)_2{\cdot}2H_2O$) were provided by Tianjin Tianli Chemical Reagent Co., Ltd and Tianjin Guangfu Fine Chemical Research Institute, respectively. H_2PtCl_6 (8 wt. % in H_2O) was ordered from Shanghai Aladdin Bio-Chem Technology Co., Ltd, China. Sodium sulfite anhydrous (Na_2SO_3) and sodium sulfate (Na_2SO_4) were purchased from Sinopharm Chemical Reagent Co., Ltd. All of the reagents were used as received without further purification.

2. The calculation of apparent quantum efficiency (AQE)

A 300 W Xenon lamp (CEL-PF300-T8) equipped with different wavelengths cutoff filters was utilized as light sources to measure the AQE of Cd@Al_2@Zn. The light intensity was obtained with an optical power meter (CEL-NP2000, CEAULIGHT, Beijing). 30 mg of sample dispersed in 20 mL of deionized water was utilized for the measurement. Taking the H_2 evolution at 420 nm wavelength for example, the wavelength-dependent AQE was calculated as follows.

The measured power density of simulated sunlight at 420 nm is 7.89 mW/cm^2. After 4 h of illumination, the total incident power (N) over the 28.3 cm^2 irradiation area (3 cm radius) is:

$$N = \frac{E\lambda}{hc} = \frac{7.89 \times 10^{-3} \times 28.3 \times 3600 \times 4 \times 420 \times 10^{-9}}{6.626 \times 10^{-34} \times 3 \times 10^{8}} = 6.79 \times 10^{21}$$

The total evolution amount of H_2 detected by gas chromatography (GC) is 1756 μmol,

$$QE = \frac{2 \times the\ number\ of\ evolved\ H_2\ molecules}{the\ number\ of\ incident\ photons}$$
$$= \frac{2 \times 6.02 \times 10^{23} \times 1756 \times 10^{-6}}{6.79 \times 10^{21}} = 31.14\ \%$$

3. Figures

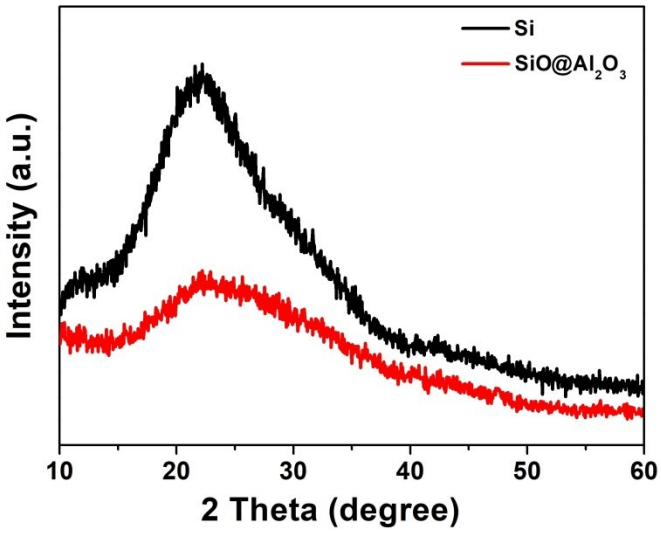

Fig. S1. XRD spectra of Si substrate before and after 200 cycles of Al_2O_3 deposition.

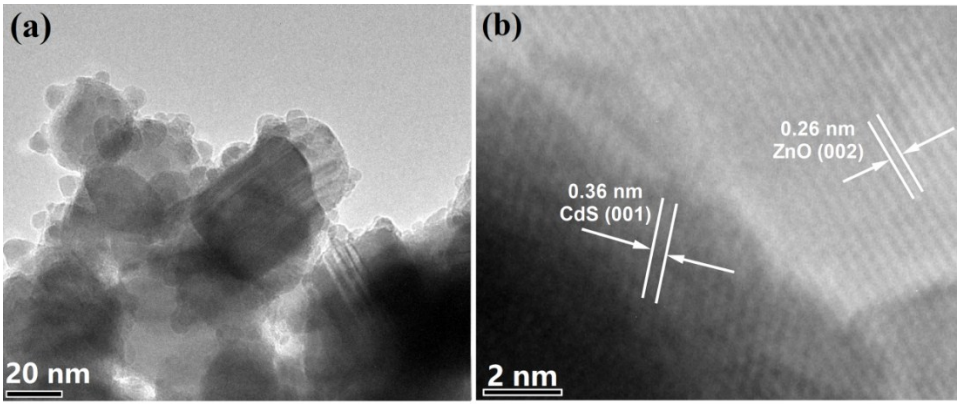

Fig. S2. TEM and HRTEM images of Cd@Zn.

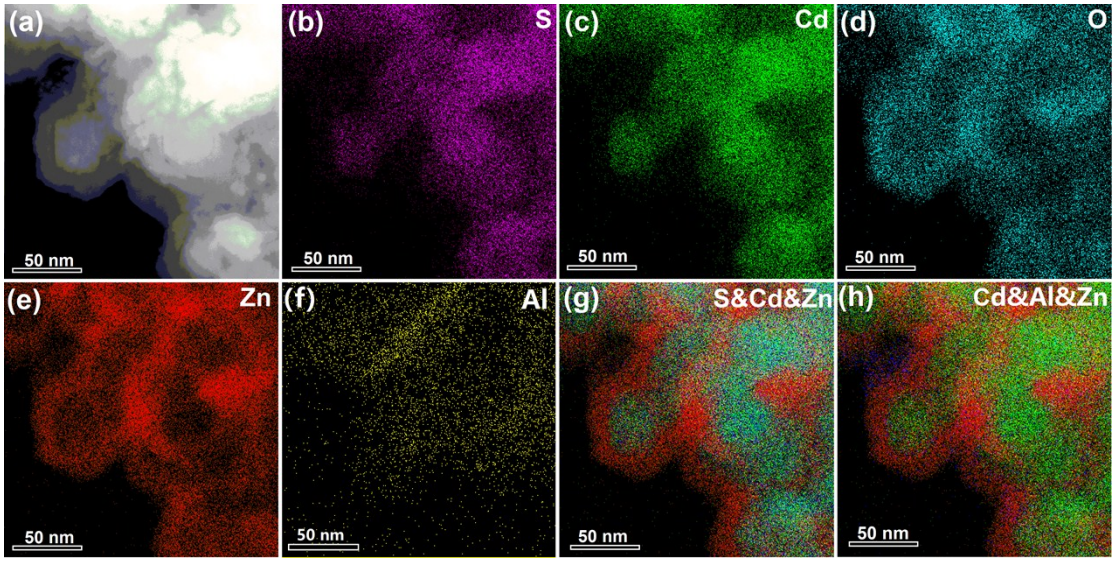

Fig. S3. (a) High-angle annular dark field-scanning transmission electron microscopy (HAADF-STEM) image and (b-f) element distribution mapping results of S, Cd, O, Zn and Al taken from Cd@Al_{10}@Zn. (g) and (h) are the overlapped mapping results of S&Cd&Zn and Cd&Al&Zn, respectively.

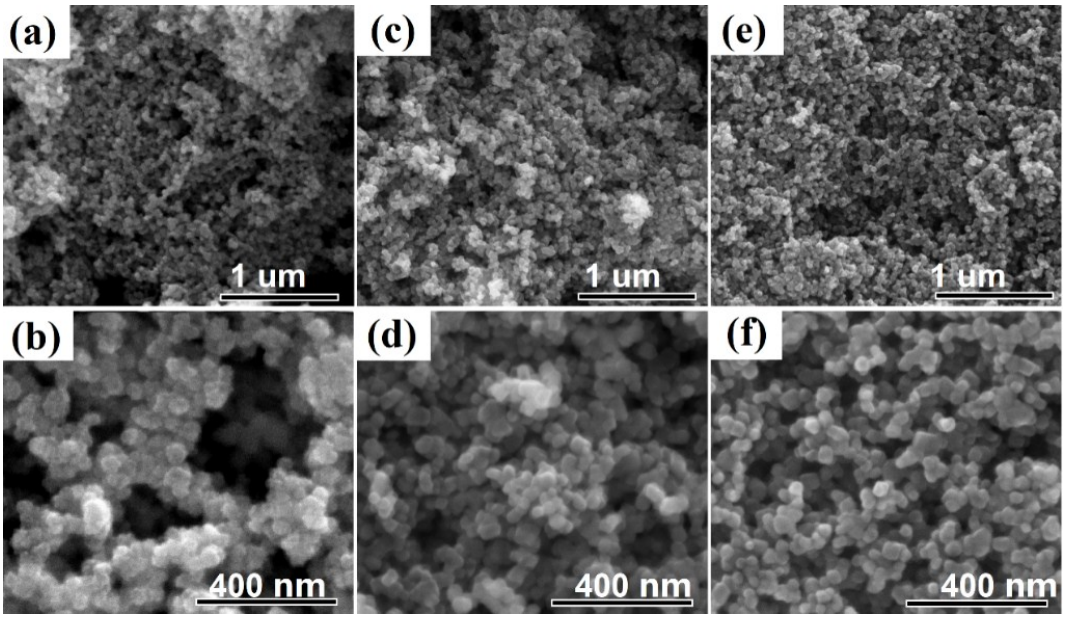

Fig. S4. SEM images of (a, b) Cd@Zn, (c, d) Cd@Al_{10} and (e, f) Cd@Al_{10}@Zn.

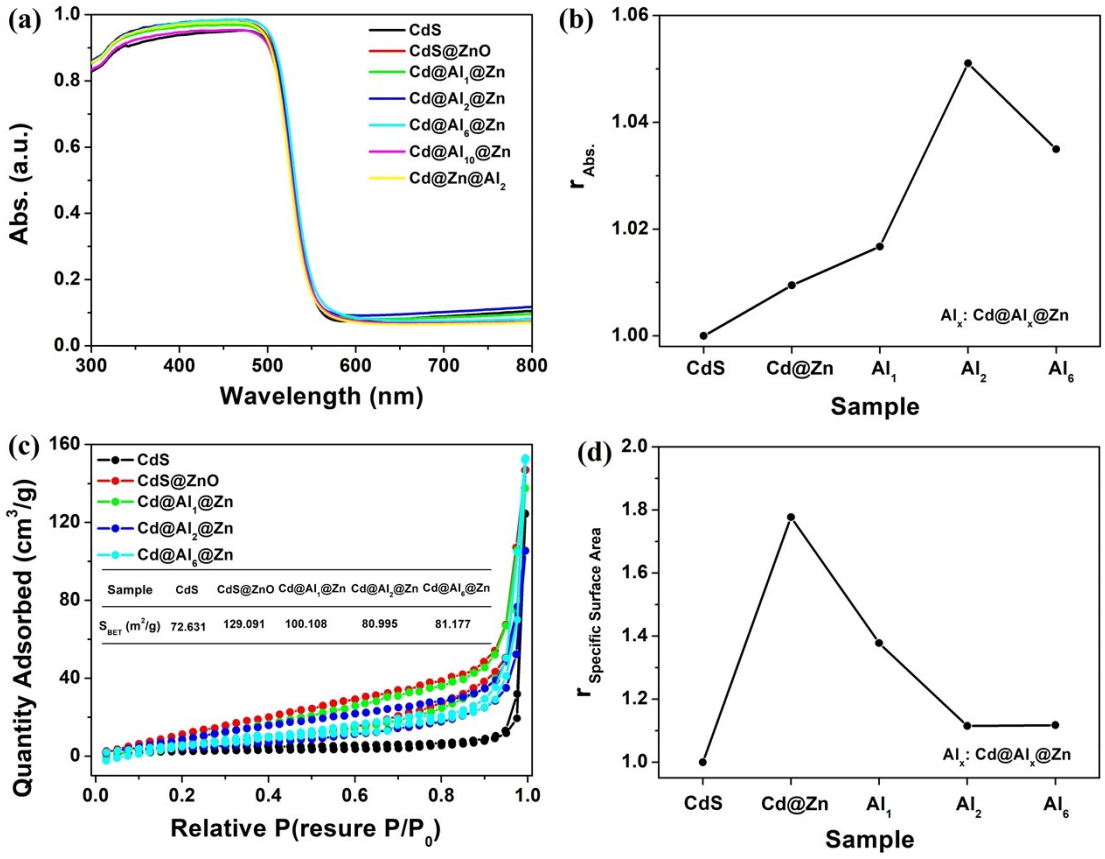

Fig. S5. (a) Light absorption spectra and (c) BET of the as fabricated samples. (b) and (d) are the relative light absorption ability and relative specific surface area normalized by using CdS as the referenced sample.

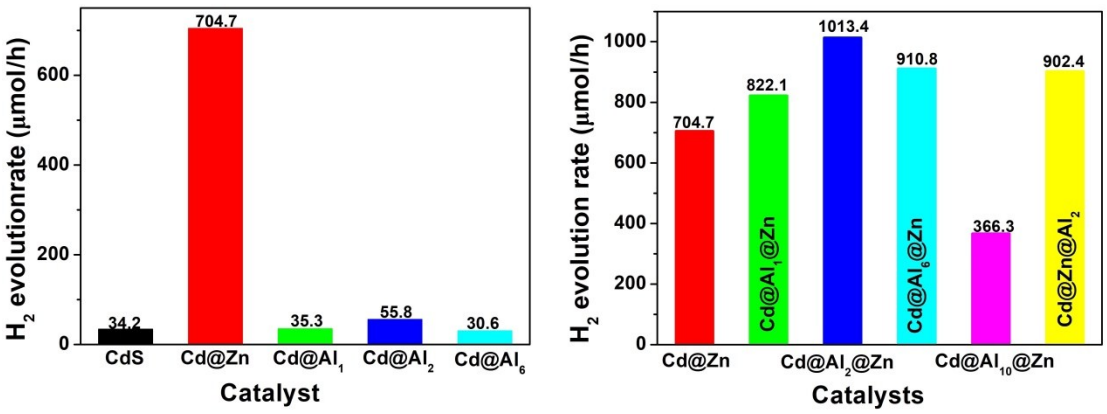

Fig S6. The comparison of photocatalytic H_2 generation rates over the as-fabricated samples, the amount of catalysts is 10 mg, all of the data were obtained without normalization.

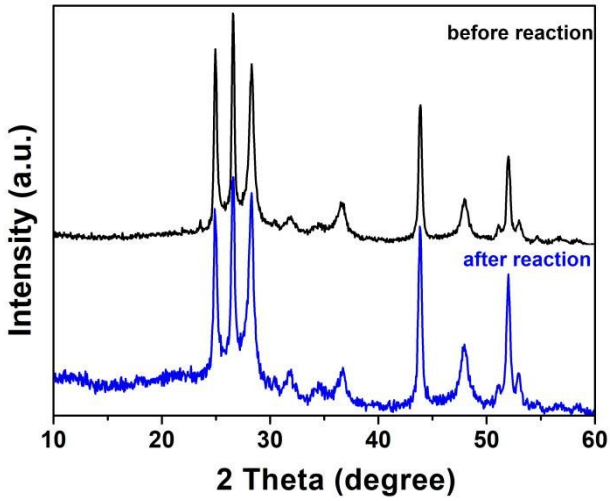

Fig. S7. XRD spectra of Cd@Al_2@Zn before and after 20 h reaction for 4 cycles.

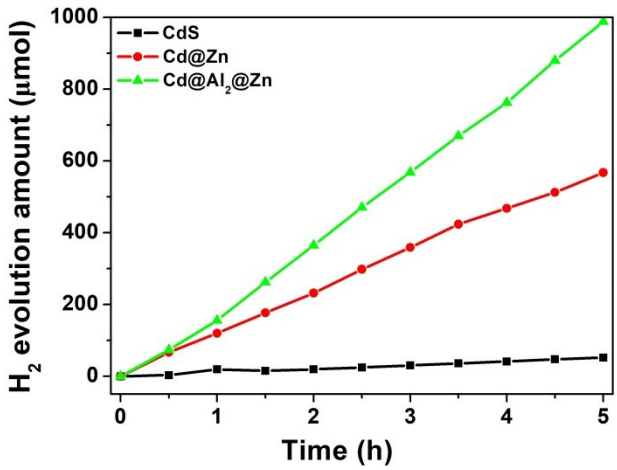

Fig. S8. H_2 evolution amount as a function of time over CdS, Cd@Zn and Cd@Al_2@Zn catalysts in the absence of Pt cocatalyst.

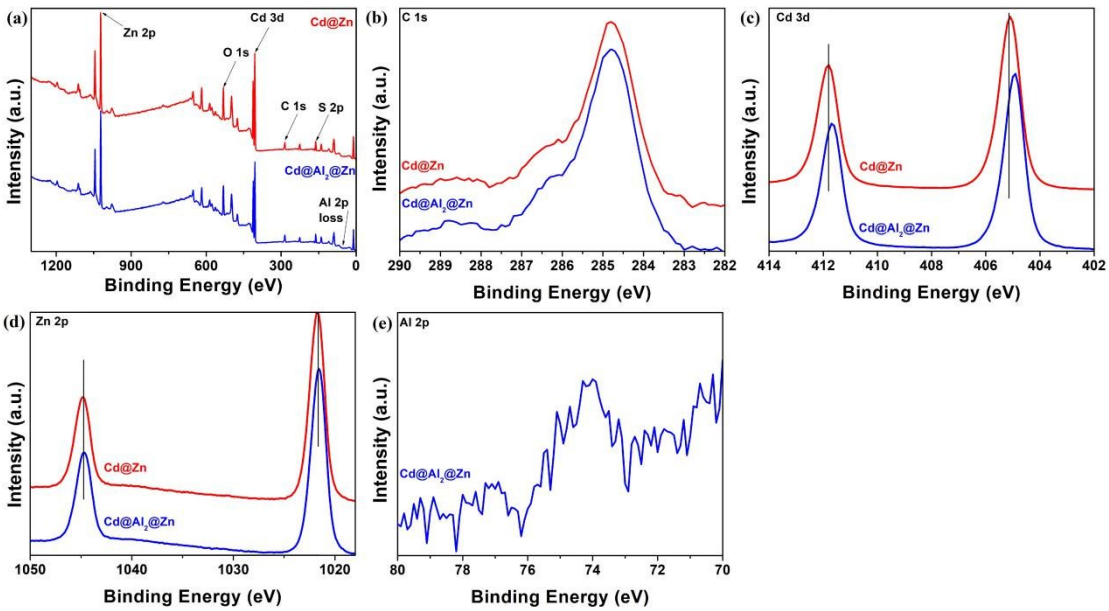

Fig. S9. XPS spectra of Cd@Zn and Cd@Al_2@Zn : (a) Survey, (b) C 1s, (c) Cd 3d, (d) Zn 2p and (e) Al 2p.

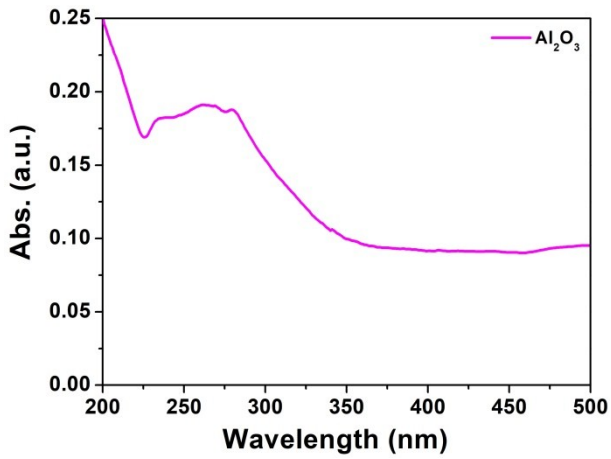

Fig. S10. UV-vis absorption spectrum of pure Al_2O_3 prepared by ALD method.

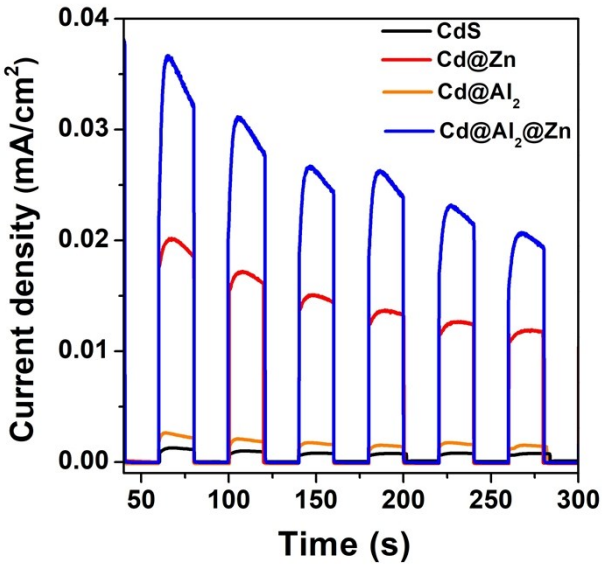

Fig. S11. (a) Photocurrent-time (i-t) curves of CdS, Cd@Zn, Cd@Al_2 and Cd@Al_2@Zn.

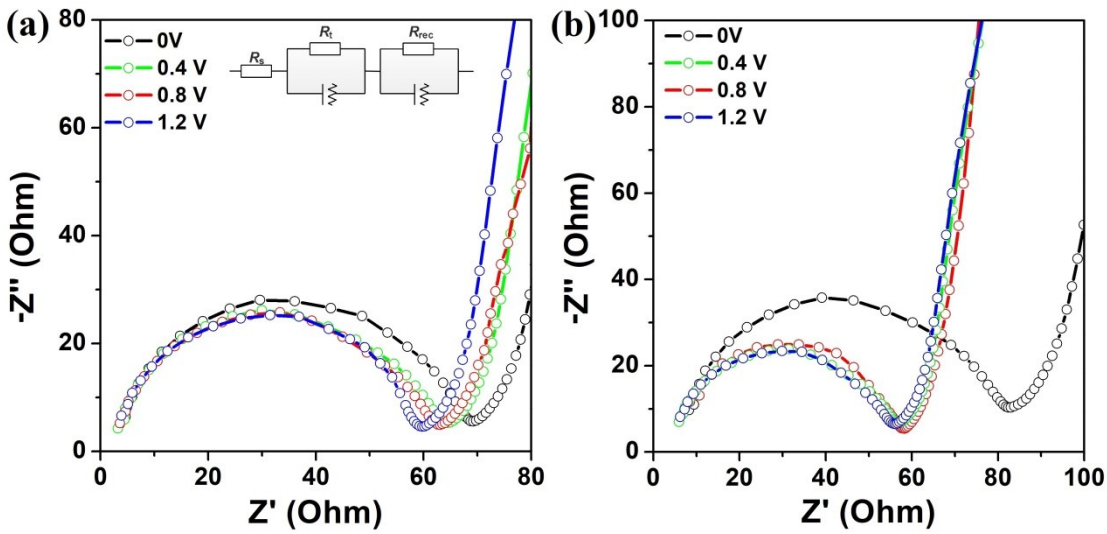

Fig. S12. EIS curves of (a) Cd@Zn and (b) Cd@Al_2@Zn measured at different applied bias voltage under 300 W Xe lamp irradiation (the inset is the equivalent circuit diagram).

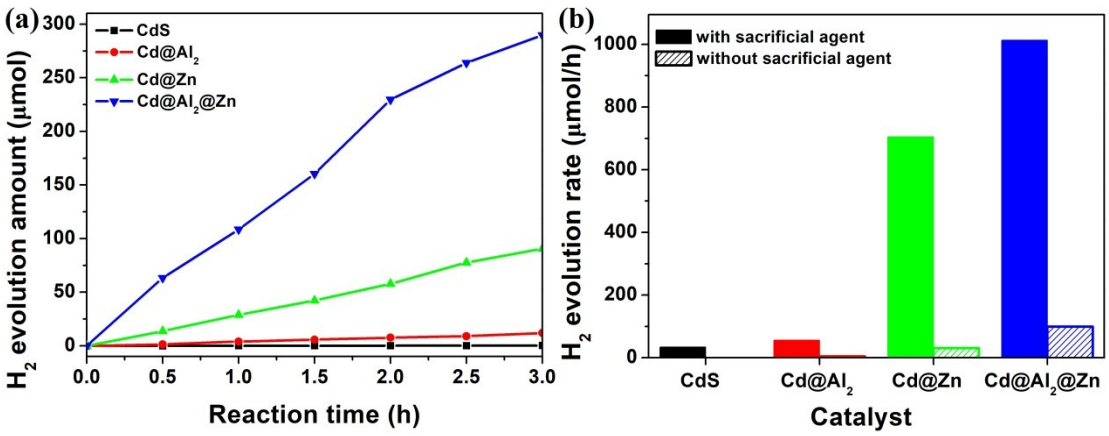

Fig. S13. (a) H_2 evolution amount as a function of time with the absence of sacrificial agent. (b) Comparison of H_2 evolution rate with and without the addition of extra sacrificial agent.

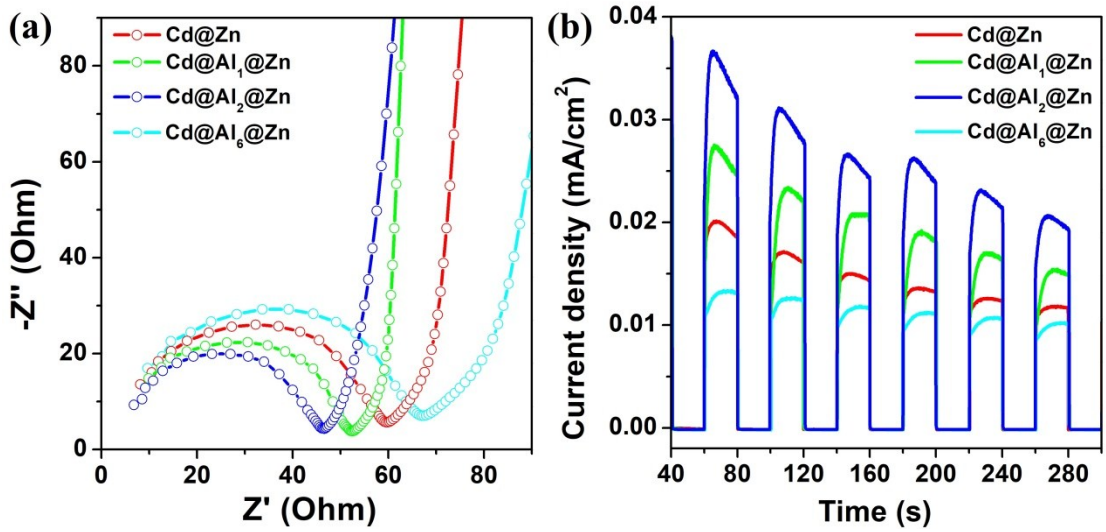

Fig. S14. (a) EIS and (b) Photocurrent-time (i-t) curves of Cd@Al_x@Zn with different deposition cycle of Al_2O_3.

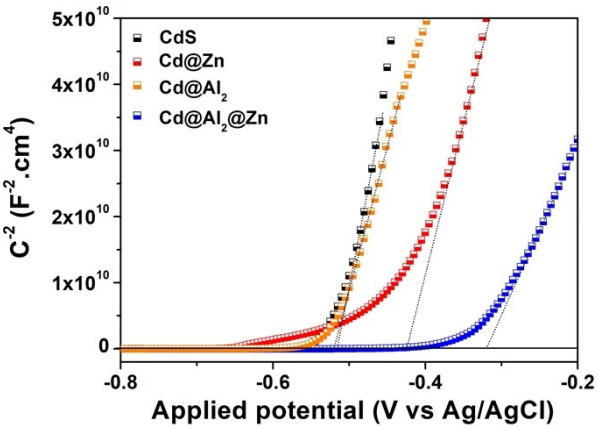

Fig. S15. Mott-Schottky plots of CdS, Cd@Zn,Cd@Al_2 and Cd@Al_2@Zn.

Tables

Table S1. The elemental composition of Cd@Zn and Cd@Al_2@Zn determined by XPS measurement.

Sample	The elemental composition (%)				
	Cd	**Zn**	**O**	**S**	**C**
Cd@Zn	19.72	10.11	36.6	10.58	22.99
Cd@Al_2@Zn	11.11	19.90	34.75	11.31	22.93

Table S2. Compassion of different H_2 evolution enhancement strategies over the CdS-ZnO based heterostructure with the addition of cocatalyst.

catalyst	Cocatalyst	light source	*R(H_2)* (mmol/g/h)	reference
CdS@Al_2O_3@ZnO	Pt	225W Xe lamp	101.3	this work
ZnO-CdS/RGO	Pt	300W Xe lamp	11.2	[1]
ZnS-CdS/GO	Pt	300 W Xe lamp	16.8	
ZnO/Pt/CdS	Pt	400W Xe lamp	17.4	[2]
ZnO/CdS/RGO	Pt	300W Xe lamp	5.9	[3]
ZnO/Pt/CdS	Pt	400 W Xe lamp	6.9	[4]
ZnO-Au-CdS	Au	300W Xe lamp	0.61	[5]
ZnS/CdS/ZnO	Pt	225W Xe lamp	44.7	[6]
CdS-Au/ZnO	Au	300 W Xe lamp	2.08	[7]
CdS/Au/ZnO	Au	300 W Xe lamp, visible light	5.2	[8]
ZnO-CdS@Cd	Pt	300 W Xe lamp	19.2	[9]

Table S3. Comparison of the interlayer passivation effect in the utilization of different fields.

catalyst	Cocatalyst	performance enhancement after passivation	reference
CdS@**Al_2O_3**@ZnO	Pt	2.2 times higher photocatalytic H_2 evolution rate	this work
CdSe/**Al_2O_3**/TiO_2	--	1.2 times higher photoelectrocatalytic H_2 evolution rate	[10]
ITO/NiO/**Al_2O_3**/Si/ZnO/Ag	Ag	9 times higher external quantum efficiency of PL	[11]
ZnO/**Al_2O_3**/GaN	Au	3 times enhanced turn-on voltage	[12]
n-ZnO/**Al_2O_3**/p-Si	--	1.6 times higher PL intensity	[13]
$NiCrAlY_3$/**Al_2O_3**/Ti_2AlNb	--	1.3 times higher critical load	[14]
Graphene/**Al_2O_3**/Si	Au	2.3 times higher photo-conversion efficiency	[15]
NiO_x/**Al_2O_3**/n-Si	--	7 times higher current density of water oxidation	[16]
Au/**Al_2O_3**/TiO_2	Au	7 times higher CO_2 reduction efficiency	[17]
TiO_2/**Al_2O_3**/ZrO_2	--	1.3 times higher power conversion efficiency	[18]
TiO_2/**Al_2O_3**/CdS	--	1.3 times higher power conversion efficiency	[19]
MoS_2/**Al_2O_3**/g-C_3N_4	--	1.65 times higher photocatalytic H_2 evolution rate	[20]
ITO/**ZnO**/$PC_{71}BM$	--	3 times higher water oxidation ability	[21]
GaAs/**ZnO**/HfO_2	--	1.7 times higher capacitance	[22]
FTO/**ZnO**/TiO_2/$CuInS_2$	--	1.2 times higher photovoltaic conversion efficiency	[23]
Fe_2O_3/**$Fe_xSn_{1-x}O_4$**/FeOOH	--	1.2 times higher photocurrent density	[24]

Reference

[1] X. Wang, L. Yin and G. Liu, *Chem. Commun.*, 2014, **50**, 3460-3463.

[2] S. R. Lingampalli, U. K. Gautam, C. N. R. Rao, *Energy Environ. Sci.*, 2013, **6**, 3589-3594.

[3] X. Wang, X. Yao, *Carbon*, 2014, **77**, 667-674.

[4] A. Roy, S. R. Lingampalli, S. Saha and C. N. R. Rao, *Chem. Phys. Lett.*, 2015, **637**, 137-142.

[5] T. Zhuang, Y. Liu, Y. Li, M. Sun, Z. Sun, P. Du, J. Jiang, S. Yu, *Small*, 2017, **13**, 1602629.

[6] J. Shi, D. Ma, Y. Zou, Z. Fan, J. Shi, L. Cheng, X. Ji, C. Niu, *J. Power Sources*, 2018, **379**, 249-260.

[7] Z. B. Yu, Y. P. Xie, G. Liu, G. Q. M. Lu, X. L. Ma, H. Cheng, *J. Mater. Chem. A*, 2013, 1, 2773-2776.

[8] S. Liang, B. Han, X. Liu, W. Chen, M. Peng, G. Guan, H. Deng, Z. Lin, *J. Alloys. Compounds*, 2018, **754**, 105-113.

[9] X. Wang, G. Liu, L. Wang, Z. Chen, G. Lu, H. Cheng, *Adv. Energy. Mat.*, 2012, **2**, 42-46.

[10] Y. Wang, W. Bai, H. Wang, Y. Jiang, S. Han, H. Sun, Y. Li, G. Jiang, Z. Zhao, Q. *Dalton Trans.*, 2017, **46**, 10734-10741.

[11] S. Zhao, X. Liu, W. Gu, X. Liang, Z. Ni , H. Tan, K. Huang, Y. Yan, X. Yu, M. Xu, X. Pi, D. Yang, *IEEE T. Electron Dev.*, 2018, **2**, 577-583.

[12] T. Wang, H. Wu, H. Zheng, J. B. Wang, Z. Wang, C. Chen, Y. Xu, C. Liu, *Appl. Phys. Lett.*, 2013, **102**, 141912.

[13] T. Wang, H. Wu, C. Chen, C. Liu, *Appl. Phys. Lett.*, 2012, **100**, 011901.

[14] H. Q. Li, Q. M. Wang, S. M. Jiang, J. Ma, J. Gong, C. Sun, *Corros. Sci.*, 2011, **53**, 1097-1106.

[15] M. A. Rehman, I. Akhtar, W. Choi, K. A. yeshaq, F. S. Hussain, M. A. Shehzad, S. H. Chun, J. Jung, Y. Seo, *Carbon*, 2018, **132**, 157-164.

[16] M. J. Park, J. Y. Jung, S. M. Shin, J. W. Song, Y. H. Nam, D. Y. Kim, J. H. Lee, *Thin Solid Films*, 2016, **599**, 54-58.

[17] H. Zhao, X. Zheng, X. Feng, Y. Li, *J. Phys. Chem. C*, 2018, **122**, 18949-18956.

[18] Y. Xiong, X. Zhu, A. Mei, F. Qin, S. Liu, S. Zhang, Y. Jiang, Y. Zhou, H. Han, *Sol. RRL*, 2018, **2**, 1800002.

[19] A. E. Roelofs, T. P. Brennan, J. C. Dominguez, C. D. Bailie, G. Y. Margulis, E. T. Hoke, M. D. McGehee, S. F. Bent, *J. Phys. Chem. C*, 2013, **117**, 5584-5592.

[20] S.V. Prabhakar Vattikuti, C. *Byon, Mater. Res. Bull.*, 2017, **96**, 233-245

[21] L. Wang, D. Yan, D. W. Shaffer, X. Ye, B. H. Layne, J. J. Concepcion, M. Liu, C. Nam, *Chem. Mater.*, 2018, **30**, 324-335.

[22] Y. Byun, S. Choi, Y. An, P. C. McIntyre, H. Kim, *ACS Appl. Mater. Interfaces*, 2014, **6**, 10482-10488.

[23] Z. Peng, Z. Liu, J. Chen, Y. Ren, W. Li, C. Li, J. Chen, *Electrochim. Acta.*, 2019, **299**, 206-212.

[24] X. Cheng, S. Cao, Y. Huan, Z. Bai, M. Li, H. Wu, R. Zhang, W. Peng, Z. Ji, X. Yan, *Energy Technol.*, 2019, **7**, 1800899.